Water Resources Research

RESEARCH ARTICLE
10.1029/2022WR031972

Potential of Thermal Neutrons to Correct Cosmic-Ray Neutron Soil Moisture Content Measurements for Dynamic Biomass Effects

J. Jakobi[1], J. A. Huisman[1], H. Fuchs[2], H. Vereecken[1], and H. R. Bogena[1]

[1]Agrosphere Institute (IBG-3), Forschungszentrum Jülich GmbH, Jülich, Germany, [2]Wasserverband Eifel-Rur (WVER), Düren, Germany

Key Points:

- Cosmic ray soil moisture measurements were most accurate when corrected with in-situ biomass measurements or thermal neutron intensity
- The effect of biomass on epithermal and thermal neutron intensity is plant-specific
- Biomass could be estimated from thermal neutron intensity for three crops, but not with the thermal-to-epithermal neutron ratio

Supporting Information:

Supporting Information may be found in the online version of this article.

Correspondence to:

H. R. Bogena,
h.bogena@fz-juelich.de

Citation:

Jakobi, J., Huisman, J. A., Fuchs, H., Vereecken, H., & Bogena, H. R. (2022). Potential of thermal neutrons to correct cosmic-ray neutron soil moisture content measurements for dynamic biomass effects. *Water Resources Research*, *58*, e2022WR031972. https://doi.org/10.1029/2022WR031972

Received 11 JAN 2022
Accepted 25 JUL 2022

Author Contributions:

Conceptualization: J. Jakobi, J. A. Huisman, H. R. Bogena
Data curation: H. R. Bogena
Formal analysis: J. Jakobi
Funding acquisition: H. R. Bogena
Investigation: J. Jakobi, H. R. Bogena
Methodology: J. Jakobi, J. A. Huisman, H. R. Bogena
Project Administration: H. R. Bogena
Resources: H. Fuchs, H. R. Bogena
Software: J. Jakobi

Abstract Cosmic-ray neutron sensors (CRNS) enable noninvasive determination of field-scale soil moisture content by exploiting the dependence of the intensity of aboveground epithermal neutrons on the hydrogen contained in soil moisture. However, there are other hydrogen pools besides soil moisture (e.g., biomass). Therefore, these hydrogen pools should be considered for accurate soil moisture content measurements, especially when they are changing dynamically (e.g., arable crops, deforestation, and reforestation). In this study, we test four approaches for the correction of biomass effects on soil moisture content measurements with CRNS using experiments with three crops (sugar beet, winter wheat, and maize) based on high-quality reference soil moisture: (a) site-specific functions based on in-situ measured biomass, (b) a generic approach, (c) the thermal-to-epithermal neutron ratio (N_r), and (d) the thermal neutron intensity. Bare soil calibration of the CRNS resulted in high root mean square errors (RMSEs) of 0.097, 0.041, and 0.019 m³/m³ between estimated and reference soil moisture content for sugar beet, winter wheat, and maize, respectively. Considering in-situ measured biomass for correction reduced the RMSE to 0.015, 0.018, and 0.009 m³/m³. The consideration of thermal neutron intensity for correction was similarly accurate. We also explored the use of CRNS for biomass estimation and found that N_r only provided accurate biomass estimates for sugar beet. In contrast, we found significant site-specific relationships between biomass and thermal neutron intensity for all three crops, suggesting that thermal neutron intensity can be used both to improve CRNS-based soil moisture content measurements and to quantify crop biomass.

Plain Language Summary Water availability is a key challenge in agriculture, especially given the expected increase of droughts related to climate change. A promising noninvasive technique to monitor soil moisture content is cosmic-ray neutron sensing (CRNS), which is based on the negative correlation between the number of near-surface fast neutrons originating from cosmic radiation and the amount of hydrogen stored as soil moisture. However, hydrogen is also stored in other pools, such as biomass. These additional pools of hydrogen must be considered to accurately determine soil moisture content with CRNS. In this study, we used data from three experiments with different crops for comparing four methods for the correction of biomass effects on the measurement of soil moisture content with CRNS. We found that soil moisture content measurements were most accurate when locally measured biomass was considered for correction. We also found that changes in the amount of biomass of different crops can be quantified using thermal neutrons additionally detected by CRNS, that is, neutrons from cosmic rays that have a lower energy than fast neutrons. A correction of biomass effects using thermal neutron measurements also provided accurate soil moisture content measurements.

1. Introduction

Cosmic ray neutron sensing is a noninvasive method for soil moisture content measurement (Zreda et al., 2008). It has become a widely used method for soil moisture content determination and cosmic-ray neutron sensors (CRNS) are operated in more than 200 locations worldwide (Andreasen, Jensen, Desilets, Franz, et al., 2017; Bogena et al., 2015), also in regional (e.g., Baatz et al., 2014; Bogena et al., 2018), national (e.g., Cooper et al., 2021; Zreda et al., 2012) and continent-wide networks (e.g., Bogena et al., 2021; Hawdon et al., 2014). The aboveground epithermal neutron intensity (energy range from ~0.5 eV to 100 keV; Zreda et al., 2008) is inversely related to the hydrogen content of the environment. Since hydrogen is mostly located in soil water in terrestrial environments, measurement of the aboveground epithermal neutron intensity can be used to estimate

Supervision: J. A. Huisman, H. Vereecken, H. R. Bogena
Validation: J. Jakobi
Visualization: J. Jakobi
Writing – original draft: J. Jakobi
Writing – review & editing: J. A. Huisman, H. Fuchs, H. Vereecken, H. R. Bogena

soil moisture content (Desilets et al., 2010). The sensing volume of CRNS is much larger than other ground-based soil moisture sensing techniques and corresponds to a cylinder with 130–240 m radius and 15–83 cm soil depth depending on the soil moisture content (Köhli et al., 2015; Schrön et al., 2017).

It is important to note that hydrogen is also stored in other environmental pools besides soil, which may cause deviations between soil moisture content determined with CRNS and reference measurements. Common additional hydrogen sources are snow (Bogena et al., 2020; Tian et al., 2016), biomass (Baatz et al., 2015; Baroni & Oswald, 2015; Fersch et al., 2018; Franz, Zreda, Rosolem, et al., 2013; Jakobi et al., 2018; Tian et al., 2016), ponding water (Schrön et al., 2017), and interception by vegetation (Andreasen et al., 2016; Baroni & Oswald, 2015; Jakobi et al., 2018) as well as the litter layer (Bogena et al., 2013). The timing of the observed deviations may help to identify the most probable source of additional hydrogen affecting the epithermal neutron intensity. In the absence of snow, earlier CRNS sensing studies on agricultural sites typically identified biomass as the most important reason for deviations between the CRNS-derived soil moisture content and in-situ measured reference soil moisture content (e.g., Baroni & Oswald, 2015; Jakobi et al., 2018; Tian et al., 2016). Thus, the removal of the effect of biomass is crucial for accurate soil moisture content estimation especially on agricultural sites. Although methods to correct soil moisture content for the presence of biomass have been developed (e.g., Baatz et al., 2015; Hawdon et al., 2014; Jakobi et al., 2018), they typically require laborious biomass measurements that are often not available.

To circumvent the need for laborious biomass measurements, several studies attempted to directly determine the amount of aboveground biomass from epithermal CRNS measurements and in-situ soil moisture content measurements (Baroni & Oswald, 2015; Franz, Zreda, Rosolem, et al., 2013). More recently, it was shown that the ratio of thermal (≤0.5 eV) to epithermal neutron intensity (N_r) can be used to determine aboveground biomass and to correct biomass effects on CRNS measurements (Jakobi et al., 2018; Tian et al., 2016). The dependency of N_r on biomass was also confirmed by neutron transport modeling of a forest site (Andreasen, Jensen, Desilets, Zreda, et al., 2017) and by a comparison of the measured N_r with vegetation indices derived from remote sensing (Vather et al., 2020). However, no detailed investigations have been undertaken as to why N_r depends on biomass and whether N_r-based correction methods can be applied for different vegetation types. Such investigations are particularly important given that the intensity of thermal neutrons also depends on soil moisture content and soil chemistry, since thermal neutrons are particularly strongly absorbed by certain elements in the soil (Andreasen et al., 2016; Zreda et al., 2008). In addition, recent studies have shown that the sensing volume of thermal neutrons is much smaller than in the case of epithermal neutrons (Bogena et al., 2020; Rasche et al., 2021). Using neutron transport simulations, it was found that thermal neutrons have a radial footprint of approximately 45 m, which increases only slightly with soil moisture content, and a sensing depth that increases from 10 to 65 cm with decreasing soil moisture content from 0.50 to 0.01 m^3/m^3 (Jakobi et al., 2021).

The aim of this study was to test four approaches for the correction of crop biomass effects on CRNS soil moisture content measurements for three crops (sugar beet, maize, and winter wheat) based on high-quality reference soil moisture content datasets. In particular, we considered the following approaches for correction: (a) local linear regression models based on epithermal neutron intensity, in-situ soil moisture content, and in-situ biomass measurements, (b) the empirical generic approach developed by Baatz et al. (2015), (c) local linear regression models based on both epithermal neutron and N_r measurements, and (d) local linear regression models based on both epithermal neutron and thermal neutron measurements. In addition, we evaluated to what extent aboveground biomass can be determined from the N_r and from the thermal neutron intensity for the three crops considered in this study.

2. Materials and Methods

2.1. The Selhausen Experimental Site

The Selhausen experimental site is located in western Germany, approximately 40 km west of Cologne (50.865°N, 6.447°E) and is part of the TERENO (TERrestrial ENvironmental Observatories) Rur hydrological observatory (Bogena et al., 2018). The site is located in the temperate maritime climate zone with a mean annual temperature and precipitation of 10.2°C and 714 mm, respectively (Korres et al., 2015). The experimental site consists of 52 fields managed by local farmers. The main soil type is Cambisol with a silty loam soil texture (Brogi et al., 2019; Rudolph et al., 2015) on top of Pleistocene sand and gravel sediments interrupted by subsurface channels of the

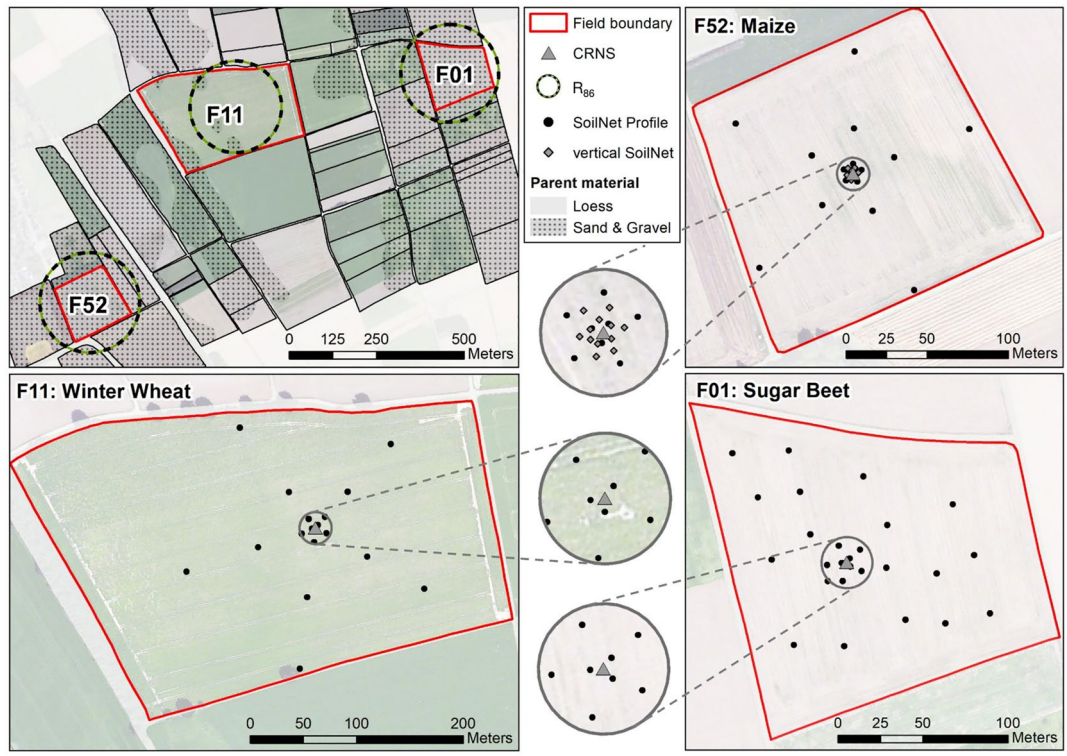

Figure 1. Map of the Selhausen experimental site showing an overview of the fields with dominant parent material and the footprint radii (R_{86}) of the three experiments estimated using the average soil moisture content, air humidity, pressure, and vegetation height conditions, respectively (i.e., winter wheat: 132 m; sugar beet: 157 m; and maize: 146 m). Furthermore, the SoilNet locations within the three fields and magnifications with 15 m radius around the cosmic-ray neutron sensor (CRNS) are shown for winter wheat and sugar beet. For the maize experiment, the magnification shows an area with a 10 m radius around the CRNS. Base maps: ESRI World Imagery and Contributors.

Rhine/Meuse river system filled with finer sediment (Weihermüller et al., 2007). This subsoil heterogeneity leads to characteristic biomass patterns, especially on the sand and gravel-dominated fields (compare Figure 1; Brogi et al., 2020; Rudolph et al., 2015). The experiments presented in this study were conducted on three different fields (Figure 1) with three different crops and in 3 years: winter wheat on field F11 in 2015 (Fuchs, 2016), sugar beet on field F01 in 2016 (Jakobi et al., 2018), and maize on field F52 in 2018.

2.2. Auxiliary Meteorological Data

Air temperature, relative humidity, and atmospheric pressure were measured on-site during the experiments. The absolute humidity necessary for neutron count correction was calculated from relative humidity and air temperature. Data gaps in absolute humidity and atmospheric pressure were filled based on linear regression models obtained for the entire measurement period. For this, time series of the same variables were obtained from a climate station situated next to the CRNS on field site F11 (SE_EC_001, http://teodoor.icg.kfa-juelich.de/ibg3searchportal2/index.jsp, compare Figure 1). Hourly precipitation sums were obtained from a nearby climate station ~400 m northeast of the field site F11 (SE_BDK_002).

2.3. In-Situ Soil Moisture Content Measurements

We used SoilNet wireless sensor networks (Bogena et al., 2010) for obtaining reference in-situ soil moisture content at 18–26 locations within each field (Figure 1). At each location, soil moisture content was measured at three depths using two soil moisture content sensors (sugar beet and maize: SMT100, Truebner GmbH, Neustadt, Germany; winter wheat: SPADE, sceme.de GmbH, Horn-Bad Meinberg, Germany). Two sensors were installed at each depth to increase the measurement volume and to identify malfunctioning sensors. Each sensor was

calibrated individually to translate the sensor response into dielectric permittivity (Bogena et al., 2017). The measured permittivity was related to soil moisture content with the Topp et al. (1980) equation. Please note that the in-situ soil moisture sensors were not corrected for variations in soil temperature and electrical conductivity which might have led to additional uncertainty in the reference soil moisture measurements.

The measurement designs at the three field sites varied because of the differently sized fields and to account for the high soil heterogeneity in the case of sugar beet (Jakobi et al., 2018). For winter wheat, we installed sensors at five locations at distances of 11, 50, and 110 m from the CRNS (i.e., 15 locations), as suggested by Schrön et al. (2017). Additionally, sensors were installed at three locations at 3 m distance from the CRNS to account for the higher sensitivity near the detector. At all locations, the measurement depths were 5, 10, and 20 cm. For sugar beet, 18 locations with measurement depths of 5, 20, and 50 cm were distributed in the field. Additionally, sensors were installed at three locations at 3 m distance and at five locations at 11 m distance from the CRNS. For these locations, the measurement depths were 5, 10, and 20 cm (Jakobi et al., 2018). For maize, sensors were installed at 18 locations at distances of 2, 6, 25, and 80 m from the CRNS. At 2 m distance, sensors were installed at three locations. At the other distances, sensors were installed at five locations. For all 18 locations, the measurement depths were 5, 15, and 30 cm. For this experiment, we additionally installed 12 SMT100 sensors vertically at distances of <5 m from the CRNS to determine the integral soil moisture content from 0 to 10 cm depth (Figure 1) to account for the sensitivity of CRNS measurements to soil moisture content changes at shallow depths (Franz et al., 2012; Köhli et al., 2015; Schrön et al., 2017).

2.4. In-Situ Soil Sampling

Additional hydrogen pools in the soil (θ_{off} [g/g]) modify the dependency of epithermal neutrons on soil moisture content (Zreda et al., 2012) and reduce the effective sensing depth of CRNS (e.g., Franz et al., 2012). We determined θ_{off} alongside bulk density (ϱ_{bd} [g/cm^3]) from soil samples of 30 cm length and 5 cm diameter obtained using a HUMAX soil corer (Martin Bruch AG, Rothenburg, Switzerland). Soil samples were taken at all SoilNet locations except for the 12 vertically inserted SMT100 sensors. For obtaining ϱ_{bd}, the soil cores were divided into 5 cm segments and oven-dried at 105°C for 24 hr. Subsequently, the soil samples were sieved and depth-specifically mixed for each field. Subsamples of 20 mg were taken from these bulk samples and heated to 1,000°C to obtain θ_{off} from the weight loss using the stoichiometric ratio of oxygen to hydrogen in H_2O (i.e., ~7.94). In this case, θ_{off} contains lattice water (LW [g/g]) and soil organic carbon (SOC [g/g]), which are traditionally determined separately and summed (e.g., Scheiffele et al., 2020; Zreda et al., 2012).

2.5. Weighting of Reference Measurements

Köhli et al. (2015) showed that the footprint of epithermal neutrons varies depending on soil moisture content, air humidity, air pressure, soil bulk density, and vegetation height. These findings were extended for short distances (<1 m) by Schrön et al. (2017). In this study, we used the most recent method for vertical and horizontal weighting of in-situ reference soil moisture content measurements of which a brief description is given in the following. For a complete description of the weighting procedure, we refer to Schrön et al. (2017).

For all experiments, we first obtained the vertical weights (i.e., W_d; Schrön et al., 2017) for each SoilNet location and measurement depth. Subsequently, W_d was used to derive a vertically weighted soil moisture content for each location and measurement time. For the vertical and horizontal weighting of in-situ ϱ_{bd} and θ_{off} measurements, we used the average of the HUMAX sample depth-intervals, that is, 2.5, 7.5, 12.5, 17.5, 22.5, and 27.5 cm. For maize and winter wheat, the reference soil moisture content locations were determined following the radial sensitivity of CRNS. Thus, a horizontal weighting was already implicitly considered. To avoid a double weighting, we first averaged the measurements for each radius. Subsequently, the results for each radius were averaged to obtain the vertically and horizontally weighted reference soil moisture content ($\theta_{reference}$), ϱ_{bd}, and θ_{off}. For sugar beet, the reference measurement was weighted using the location-specific horizontal weights (i.e., W_r; Schrön et al., 2017). At each measurement time, the procedure to determine the vertical and horizontal weighting was iterated four times, which was sufficient to reach convergence.

2.6. Biomass Measurements

During the winter wheat, maize, and sugar beet experiments, we sampled aboveground and belowground biomass at eight, five, and nine locations, respectively. At least four measurement locations were sampled in <20 m distance from the CRNS. At each sampling location, 1 m of row was harvested, sealed air-tight, and transported to the laboratory. Here, soil residues were removed and samples were split into above- and belowground biomass, and subsequently weighed and oven-dried at ≤105°C until a constant weight was reached. Due to limited oven capacity, subsamples of ∼20% of the original sample weight were occasionally used. Areal average moist and dry aboveground and belowground biomass was calculated using the arithmetic mean of all samples. As suggested by Franz, Zreda, Rosolem, et al. (2013), we assumed that the water equivalent contained in biomass (*BWE* [mm]) can be approximated by the sum of the weight loss from oven-drying and the stoichiometric amount of hydrogen and oxygen contained in cellulose (f_{ew}, ∼55.6%):

$$BWE = \left[(BM_f - BM_d) + f_{ew}\, BM_d\right] \frac{1}{p_d}\, {p_w}^{-1} \tag{1}$$

where p_w is the density of water (1,000 kg/m^3), p_d is the distance between rows (m; sugar beet: 0.465 m, winter wheat: 0.12 m, maize: 0.45 m), and BM_f and BM_d are the fresh and dry biomass weights per 1 m of row (g), respectively. We used Equation 1 to determine aboveground *BWE* (BWE_a), belowground *BWE* (BWE_b), while total *BWE* (BWE_{tot}) was obtained as $BWE_a + BWE_b$.

For sugar beet and winter wheat, biomass was sampled on 11 days, respectively. However, for winter wheat, two of the belowground biomass samples were calculated from aboveground biomass information according to Baret et al. (1992). For maize, the observation period was only 3 months due to a drought-related emergency harvest and biomass was only measured on 5 days. Therefore, additional *BWE* estimates were obtained from bi-weekly leaf area index (*LAI*) measurements with an SS1 SunScan Canopy Analysis System (Delta-T Devices, Cambridge, United Kingdom). For this, we used an exponential model to relate *BWE* and *LAI* of maize:

$$BWE_{LAI} = a_1 LAI^{b1} \tag{2}$$

where a_1 and b_1 are fitting parameters and BWE_{LAI} (mm) is the *BWE* predicted from *LAI*. We fitted Equation 2 for the prediction of aboveground *BWE* ($BWE_{a,LAI}$) and belowground *BWE* ($BWE_{b,LAI}$), while total *BWE* ($BWE_{tot,LAI}$) was obtained as $BWE_{a,LAI} + BWE_{b,LAI}$. Linear interpolation was used to obtain *BWE* estimates at non-sampled times.

2.7. Cosmic Ray Neutron Measurements

We used different types of CRNS (i.e., CRS-1000, CRS-2000/B, mobile CRNS, Hydroinnova LLC, Albuquerque, NM, USA) with moderated and bare detector tubes installed at a height of 1.5–2 m. In this study, the neutrons measured by the moderated detector are referred to as epithermal neutrons (0.5 eV to 100 keV) and the neutrons measured by the bare detector are referred to as thermal neutrons (<0.5 eV). It has to be noted that the neutron intensities measured with moderated detectors are partially affected by neutrons <0.5 eV (up to ∼ 30%; McJannet et al., 2014). Similarly, bare detectors also measure some neutrons >0.5 eV (∼4%–5%; Andreasen et al., 2016). For more information on the measurement principle, we refer to Zreda et al. (2012). Fersch et al. (2020) provide an overview of the different detector types. We collocated several CRNS in all three fields and summed up the measured neutron counts to achieve higher measurement accuracy compared to a single sensor (cf. Jakobi et al., 2020). In particular, we operated 7 moderated and 3 bare neutron detectors in the sugar beet field, 8 moderated and 4 bare detectors in the winter wheat field, and 4 moderated and 3 bare detectors in the maize field.

Before aggregation, outliers were removed from the raw neutron count time series (N_{raw}) of the individual detectors, irrespective of detector type, using two filtering steps. First, extreme outliers were removed using two threshold values:

$$N_{c1} = \begin{cases} N_{raw} > 50 \dfrac{counts}{hour} \\ N_{raw} < 10 \dfrac{kilocounts}{hour} \end{cases} \tag{3}$$

Second, outliers relative to the 24 hr moving average (N_{c24m}) ± the Poissonian uncertainty (e.g., Knoll, 2010) associated to the 24 hr moving sum ($\sqrt{N_{c24s}}$) were removed:

$$N_c = \begin{cases} N_{c1} > N_{24m} - \sqrt{N_{c24s}} \\ N_{c1} < N_{24m} + \sqrt{N_{c24s}} \end{cases} \quad (4)$$

Subsequently, the filtered hourly thermal (T_c) and epithermal (E_c) neutron count rates were summed up.

The measurements of some of the thermal and epithermal detectors contained larger data gaps. We obtained scaling factors (s_f) for each experiment and each detector relative to the cumulative average count rate during times when all detectors of the same type (i.e., T_c or E_c) were working. The s_f were used to account for missing data during summation as follows:

$$\begin{aligned} E_s &= E_c \frac{1}{\sum s_f} \\ T_s &= T_c \frac{1}{\sum s_f} \end{aligned} \quad (5)$$

where E_s and T_s are the summed epithermal and thermal neutron count series adjusted for data gaps.

Corrected epithermal neutron intensities (E) were obtained from E_s by applying established correction procedures for variations in air pressure (Desilets & Zreda, 2003), incoming cosmic ray neutron intensity (Desilets & Zreda, 2001), and air humidity (Rosolem et al., 2013). For these corrections, we used the average pressure, absolute humidity, and incoming cosmic ray neutron intensity measured during each of the three experiments. The reference incoming cosmic ray neutron intensity was obtained from the neutron monitor at Jungfraujoch (JUNG; via the NMDB neutron monitor database at www.nmdb.eu). Following the experimental findings from Jakobi et al. (2018), we obtained the corrected thermal neutron intensity (T) from T_s by applying corrections for pressure and absolute humidity only.

2.8. The Thermal-to-Epithermal Neutron Ratio

Tian et al. (2016) found a positive correlation between BWE_a of maize and soy bean and the ratio of thermal to epithermal neutrons (N_r). Such a correlation was also found for the sugar beet data set used in this study (Jakobi et al., 2018). In this study, we obtained N_r according to Jakobi et al. (2018):

$$N_r = \frac{T}{E} \frac{\overline{E}}{\overline{T}} \quad (6)$$

where $\overline{E}$ and $\overline{T}$ are the arithmetic means of the epithermal and thermal neutron intensity measured during each experiment, and E and T are the 12-hourly moving averages of the epithermal and thermal neutron intensity. We used linear models for relating N_r and BWE_a (Jakobi et al., 2018):

$$BWE_{a,Nr} = a_2 Nr + b_2 \quad (7)$$

where $BWE_{a,Nr}$ is the BWE_a estimated from N_r and a_2 and b_2 are calibration parameters. We also used a linear model for relating T and BWE_{tot}:

$$BWE_{tot,T} = a_3 T + b_3 \quad (8)$$

where $BWE_{tot,T}$ is the BWE_{tot} estimated from T and a_3 and b_3 are calibration parameters.

2.9. Conversion of Neutrons to Soil Moisture Content

We obtained volumetric soil moisture content (θ) from E with a modified approach following Desilets et al. (2010), which showed good performance in several previous studies (e.g., Baatz et al., 2014; Dimitrova-Petrova et al., 2020; Dong et al., 2014; Rivera Villarreyes et al., 2011):

$$\theta = \varrho_{bd}\left(\frac{p_0}{\frac{fE}{N_0} - p_1} - p_2 - \theta_{off}\right) \tag{9}$$

where p_i (=0.0808, 0.372, and 0.115) are fitting parameters obtained from neutron transport modeling, f is a temporally variable correction factor (derived from biomass measurements, N_r, or T), and N_0 is the epithermal neutron intensity above dry soil. In this study, we obtained N_0 from the 12-hourly moving average of the epithermal neutron intensity using three different strategies:

- In calibration strategy A, a single value for N_0 (i.e., $N_{0,opt}$) was obtained using the whole reference soil moisture content time series and assuming $f = 1$ (i.e., no additional correction).
- In calibration strategy B, a single value for N_0 (i.e., $N_{0,bare}$) was obtained for the first 2 days of the reference soil moisture content observations and assuming $f = 1$. This strategy represents the typical calibration approach using campaign-style soil sampling (e.g., Zreda et al., 2012).
- In calibration strategy C, we obtained 12-hourly N_0-values using Equation 9 and assuming $f = 1$. We used the resulting N_0 time series for predicting biomass, N_r or T related effects on epithermal CRNS measurements.

For calibration strategies A and B, N_0 is obtained by minimization of the root mean square error (RMSE) between the reference and the estimated soil moisture content.

2.10. Biomass, N_r, and Thermal Neutron Corrections

We tested four regression models for obtaining the correction factor f in Equation 9 using either BWE_a (e.g., Baatz et al., 2015), BWE_{tot}, N_r (e.g., Jakobi et al., 2018), or T:

$$N_{0,BWEa} = a_4\, BWE_a + N_{0,\,BWEa=0} \tag{10}$$

$$N_{0,BWEtot} = a_5\, BWE_{tot} + N_{0,BWEtot=0} \tag{11}$$

$$N_{0,Nr} = a_6\, N_r + N_{0,Nr=0} \tag{12}$$

$$N_{0,T} = a_7\, T + N_{0,T=0} \tag{13}$$

where a_4, a_5, a_6, and a_7 [cph] are empirical factors representing the change in N_0 per mm BWE_a, mm BWE_{tot}, N_r, or T, respectively and $N_{0,BWEa=0}$, $N_{0,BWEtot=0}$, $N_{0,Nr=0}$, and $N_{0,T=0}$ represent N_0 when BWE_a, BWE_{tot}, N_r, or T, respectively equal 0. Subsequently, we derived f by assuming that the changes in estimated N_0 and epithermal neutron intensity are proportional:

$$f_{BWEa} = \left(1 + \frac{a_4}{N_{0,BWEa=0}} BWE_a\right)^{-1} \tag{14}$$

$$f_{BWEtot} = \left(1 + \frac{a_5}{N_{0,BWEtot=0}} BWE_{tot}\right)^{-1} \tag{15}$$

$$f_{Nr} = \left(1 + \frac{a_6}{N_{0,Nr=0}} N_r\right)^{-1} \tag{16}$$

$$f_T = \left(1 + \frac{a_7}{N_{0,T=0}} T\right)^{-1} \tag{17}$$

where f_{BWEa}, f_{BWEtot}, f_{Nr}, and f_T are correction factors to be used with $N_{0,BWEa=0}$, $N_{0,BWEtot=0}$, $N_{0,Nr=0}$, and $N_{0,T=0}$, respectively in Equation 9. We also obtained correction factors for BWE_a and BWE_{tot} based on the empirical

Table 1
Soil Bulk Density (ϱ_{bd}), Gravimetric Soil Moisture Content (θ_g), and Additional Hydrogen Pools in the Soil (θ_{Off}) From the HUMAX Samples Taken on May 6, 2015 for Winter Wheat, June 6, 2016 and November 4, 2016 for Sugar Beet, and May 29, 2018 for Maize

	Winter wheat			Sugar beet			Maize		
Depth [cm]	ϱ_{bd} [g/cm^3]	θ_g [g/g]	θ_{off} [g/g]	ϱ_{bd} [g/cm^3]	θ_g [g/g]	θ_{off} [g/g]	ϱ_{bd} [g/cm^3]	θ_g [g/g]	θ_{off} [g/g]
0–5	1.188	0.200	0.033	1.34	0.194	0.027	1.242	0.176	0.048
5–10	1.262	0.197	0.032	1.396	0.189	0.027	1.256	0.192	0.049
10–15	1.280	0.193	0.032	1.397	0.189	0.027	1.331	0.191	0.049
15–20	1.274	0.190	0.032	1.375	0.187	0.028	1.344	0.196	0.049
20–25	1.280	0.190	0.032	1.429	0.178	0.026	1.358	0.202	0.05
25–30	1.284	0.122	0.032	1.464	0.170	0.026	1.288	0.198	0.048
Average	1.261	0.182	0.032	1.400	0.185	0.027	1.303	0.192	0.049
Weighted	1.247	0.192	0.023	1.379	0.189	0.016	1.277	0.186	0.034

Note. Please note that the sugar beet soil sampling results differ in comparison to Jakobi et al. (2018) and Scheiffele et al. (2020), because the average of two sampling campaigns was used here, whereas the two previous studies only used the results from the campaign on June 6.

generic biomass correction model of Baatz et al. (2015), who found a reduction in epithermal neutron intensity of ∼0.5% per mm BWE_a:

$$f_{BWEa,Baatz} = 1 + BWE_a \frac{6.4}{1215} \tag{18}$$

$$f_{BWEtot,Baatz} = 1 + BWE_{tot} \frac{6.4}{1215} \tag{19}$$

where $f_{BWEa,\ Baatz}$ and $f_{BWEtot,\ Baatz}$ again are correction factors to be used in Equation 9 and the constants 6.4 and 1,215 [cph] are the reduction per mm BWE_a and N_0 when BWE_a equals 0, respectively.

3. Results

3.1. Data Overview

Table 1 provides a summary of the basic soil properties for the three cropped fields. The bulk density generally increased with depth for all three fields, while the additional hydrogen pools θ_{off} were relatively constant with depth. It was found that the weighted bulk densities were lower than the arithmetic mean due to the decreasing sensitivity of CRNS with increasing depth.

An overview of the precipitation, normalized neutron count rates, BWE, and reference soil moisture content for the three cropped fields is given in Figure 2. The minimum, average and maximum epithermal and thermal neutron intensity after correction are provided in Table 2. Figure 2e shows that the maximum BWE_b for the three crops differed strongly. Both winter wheat and maize showed relatively low maximum BWE_b values (0.89 and 0.85 mm, respectively), whereas the maximum BWE_b for sugar beet was tenfold higher (8.23 mm). For maize, BWE_a and BWE_b were derived from *LAI* using Equation 2 (Figure 3). The high R^2 (≥0.95) indicates that *LAI* was a good predictor for BWE_a and BWE_b. Therefore, we used the *LAI*-derived BWE of maize in the remainder of the manuscript.

Figure 2f shows the vertically weighted soil moisture content measured at all SoilNet locations as well as the horizontally and vertically weighted reference soil moisture content for the three crops. The average reference soil moisture content for sugar beet and maize was notably lower (∼0.17 m^3/m^3) compared to winter wheat (0.24 m^3/m^3) due to the drought conditions in 2016 and 2018.

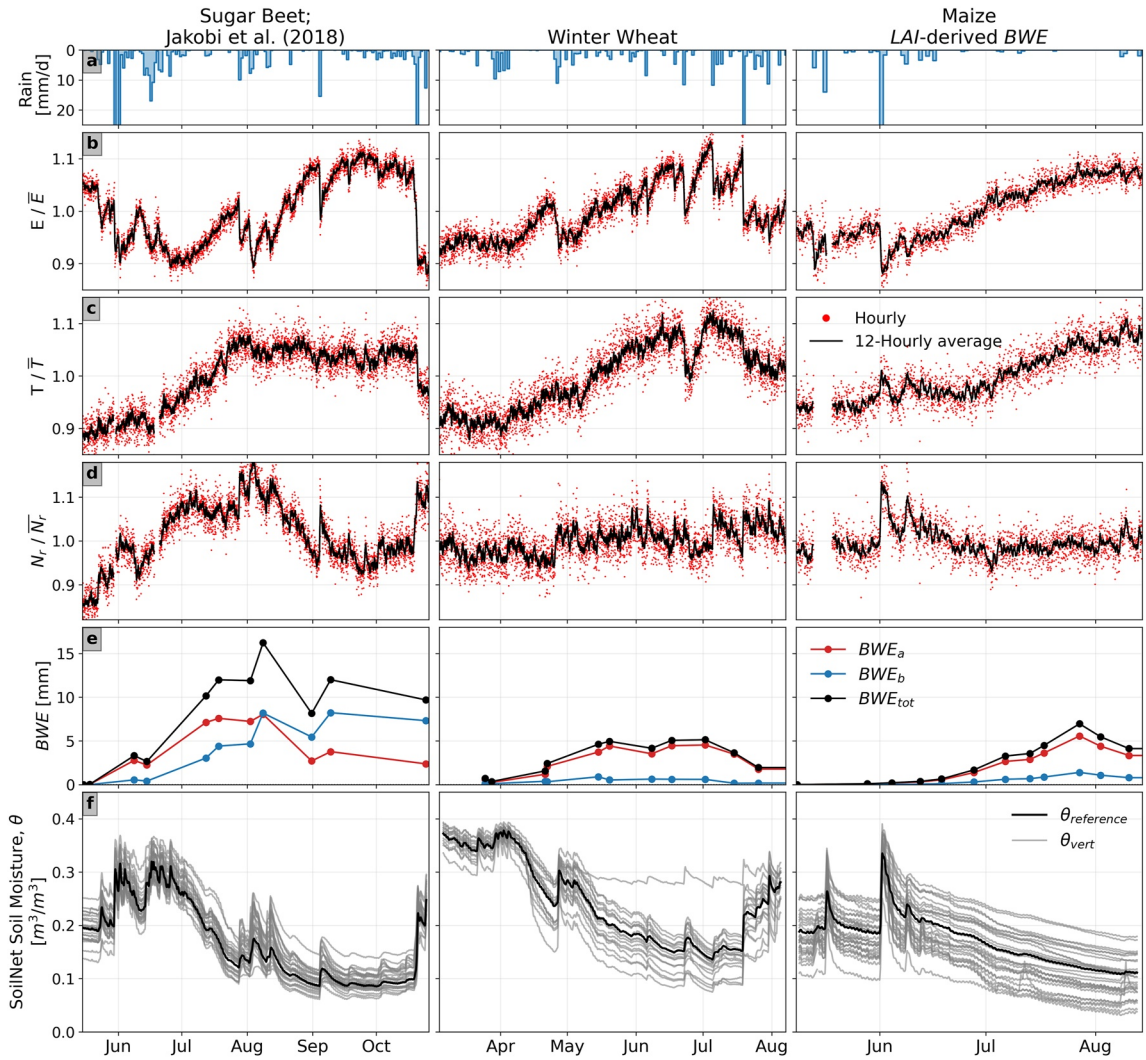

Figure 2. Time series of (a) precipitation, (b) epithermal neutron intensity (E) normalized by the average E, (c) thermal neutron intensity (T) normalized by the average T, (d) neutron ratio (N_r), (e) aboveground, belowground and total biomass water equivalent (BWE_a, BWE_b, and BWE_{tot}, respectively) and (f) soil moisture content obtained from the vertically and horizontally weighted SoilNet measurements (black, $\theta_{reference}$) and the vertically weighted SoilNet measurements (gray, θ_{vert}).

3.2. The Effect of Time-Variable Biomass on CRNS-Derived Soil Moisture Content

To investigate the influence of vegetation biomass on soil moisture content estimates with CRNS, we first calibrated N_0 during bare soil condition (calibration strategy B, Figure 4c, red). For all three crops, the soil moisture content estimated from the CRNS measurements in this way deviated from the reference soil moisture content. This was attributed to increasing biomass associated with crop growth (Figure 4c, red areas) and resulted in a

Table 2
Minimum, Average, and Maximum Corrected Epithermal and Thermal Neutron Count Rates Measured During the Experiments in Sugar Beet, Winter Wheat, and Maize Fields

	Corrected epithermal neutrons [counts/hour]			Corrected thermal neutrons [counts/hour]		
Experiment	Minimum	Average	Maximum	Minimum	Average	Maximum
Sugar beet	8,952	10,425	11,856	2,076	2,458	2,786
Winter wheat	6,063	7,350	8,542	1,296	1,562	1,849
Maize	4,248	5,273	5,868	1,877	2,148	2,499

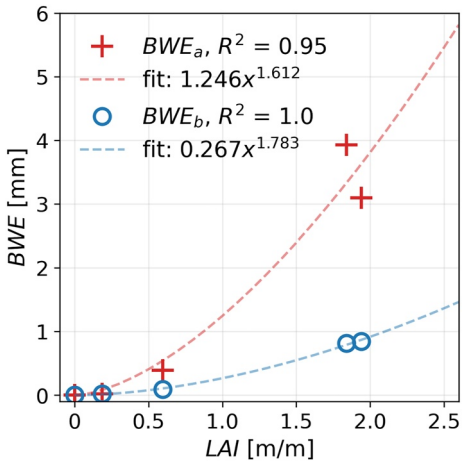

Figure 3. Relationship between leaf area index (LAI) and aboveground and belowground biomass water equivalent (BWE_a and BWE_b, respectively) for maize. The coefficients of determination (R^2) and the exponential models for predicting BWE from LAI are also provided.

high RMSE of 0.097 m^3/m^3 for sugar beet, 0.041 m^3/m^3 for winter wheat, and 0.019 m^3/m^3 for maize. For sugar beet and winter wheat, the CRNS mostly overestimated soil moisture content, indicating that the additional hydrogen in the biomass decreased the local epithermal neutron intensity. This effect was particularly strong in case of sugar beet due to its higher aboveground and belowground biomass. Interestingly, CRNS mostly underestimated soil moisture content for maize, even though the progressing growth of maize should have resulted in more neutron moderation (i.e., soil moisture content overestimation). This counterintuitive result can be explained by the fact that the atomic nuclei of the high-growing maize surrounding the CRNS acted as scattering centers that effectively increased the neutron travel paths and thus the local epithermal neutron intensity (pers. communication Markus Köhli; see also Figure 11 in Li et al., 2019). In contrast to maize, winter wheat and sugar beet did not grow tall enough in the near field of the detector, so this effect was not observed.

Figure 4c also shows the results of calibration strategy A (blue line), which considers all reference soil moisture content data but no time-variable changes in biomass. For maize and winter wheat, the reference and CRNS-derived soil moisture content showed good agreement, and the RMSE was relatively low (i.e., 0.031 m^3/m^3 for winter wheat and 0.011 m^3/m^3 for maize). For sugar beet, the visual agreement was not as good, and this was supported by the higher RMSE (0.042 m^3/m^3).

3.3. Soil Moisture Content Correction With Local Biomass Measurements

To quantify the effect of biomass on soil moisture content obtained with CRNS, we established linear regression models between the in-situ measured BWE_a and BWE_{tot} and the calibration parameter N_0 (Figure 5; also see Figure 4; please note that N_0 was normalized as $N_0/N_{0,bare}$ for these and the remaining Figures to allow easier comparison between the different crops). We found distinct differences in the N_0 – BWE relationships for the three crops. For sugar beet and winter wheat, N_0 showed a negative relationship with BWE, whereas for maize this relationship was positive for reasons already provided. For sugar beet, the slopes of the N_0 – BWE_a and N_0 – BWE_{tot} relationships differed more strongly compared to the other crops (Figure 5a), which can be explained by the higher amount of belowground biomass compared to maize and winter wheat (see also Figure 2e). In addition, the N_0 – BWE_{tot} relationship for sugar beet resulted in a higher R^2-value compared to the N_0 – BWE_a relationship,

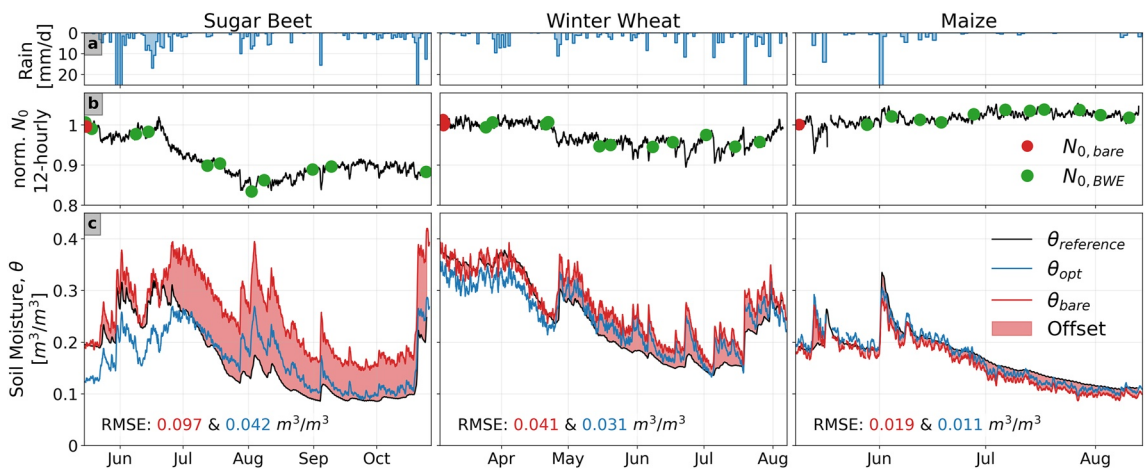

Figure 4. Time series of (a) precipitation, (b) normalized N_0 ($N_0/N_{0,bare}$), also highlighted at bare soil conditions (red) and at biomass sampling dates (green) and (c) offset between reference soil moisture content and cosmic-ray neutron sensor (CRNS)-derived soil moisture content using strategy B (i.e., bare soil calibration). CRNS-derived soil moisture content using strategy A (in blue), that is, by optimizing the entire time series of reference soil moisture content, is also shown.

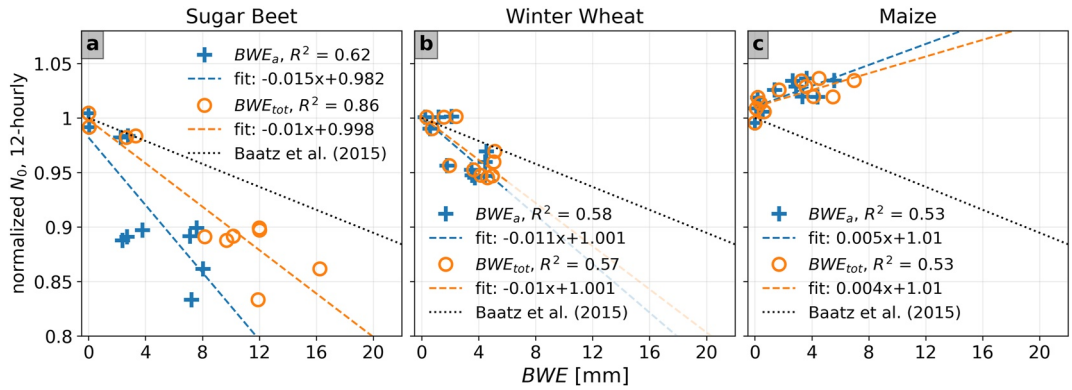

Figure 5. Scatterplots and corresponding linear regressions for predicting the change in normalized N_0 ($N_0/N_{0,bare}$) from BWE_a (blue) and BWE_{tot} (orange), respectively. The slopes of all linear fits were significantly different from 0 (i.e., the two-sided p value was <0.05 for a test with the null hypothesis that the slope is equal to 0). Additionally, the empirical model from Baatz et al. (2015) for predicting the change in normalized N_0 from BWE_a is shown.

indicating that the total biomass should be preferably used for correction in case of sugar beet. Figure 5 also shows that the relationship suggested by Baatz et al., 2015 (i.e., a reduction of ~0.5% of N_0 per mm BWE_a) was not able to represent the influence of biomass on N_0, except to some extent for winter wheat.

In a next step, the BWE_a and BWE_{tot} regression models were used for the correction of CRNS soil moisture content using Equations 14 and 15. Figure 6 shows that these corrections were able to effectively reduce the biomass effects for all three crops. In case of winter wheat and maize, a correction based on BWE_a was sufficient to obtain a low RMSE (0.018 and 0.009 m^3/m^3, respectively). In the case of sugar beet, a correction based on BWE_{tot} led to a substantially lower RMSE of 0.015 m^3/m^3 compared to 0.032 m^3/m^3 when only BWE_a was considered.

For winter wheat, the relationship of Baatz et al. (2015) showed an acceptable performance in terms of RMSE in comparison to the linear regression models (Figure 6). For sugar beet, the RMSE considering biomass correction

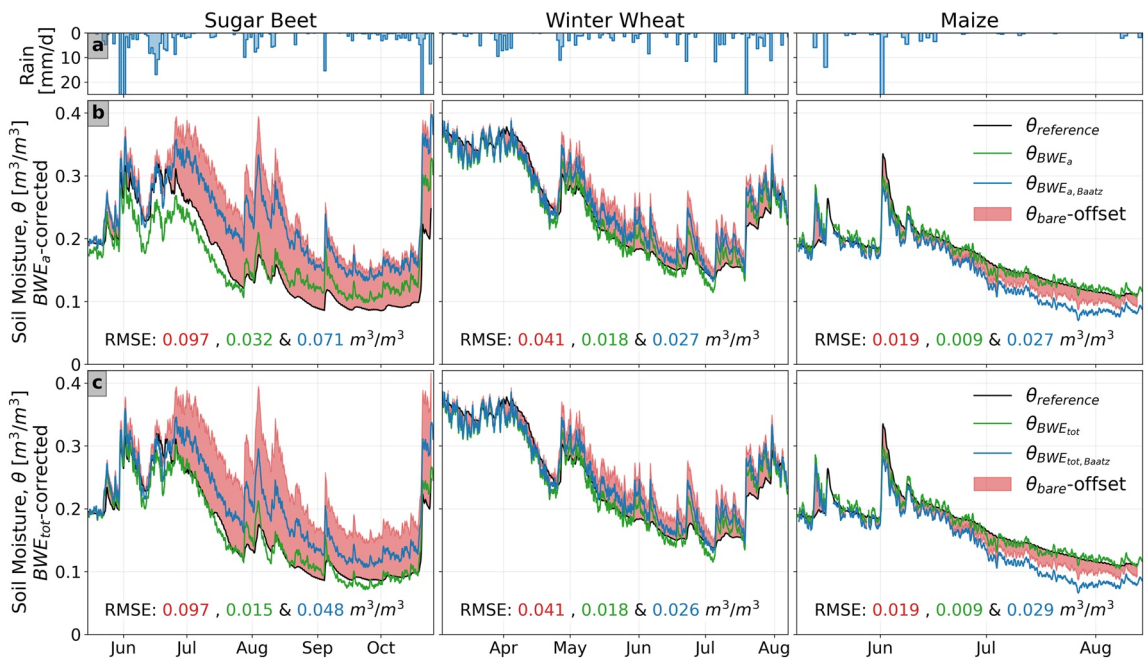

Figure 6. Times series of (a) precipitation, (b) cosmic-ray neutron sensor (CRNS)-derived soil moisture content corrected for aboveground biomass (strategy C), and (c) CRNS-derived soil moisture content corrected for total biomass (strategy C). For the biomass correction, local linear regression models (green, see Figure 5) and the empirical approach from Baatz et al. (2015) (blue) were considered. For comparison, the vertically and horizontally weighted reference soil moisture content (black) and the offset due to the bare soil calibration (red, strategy B) are shown.

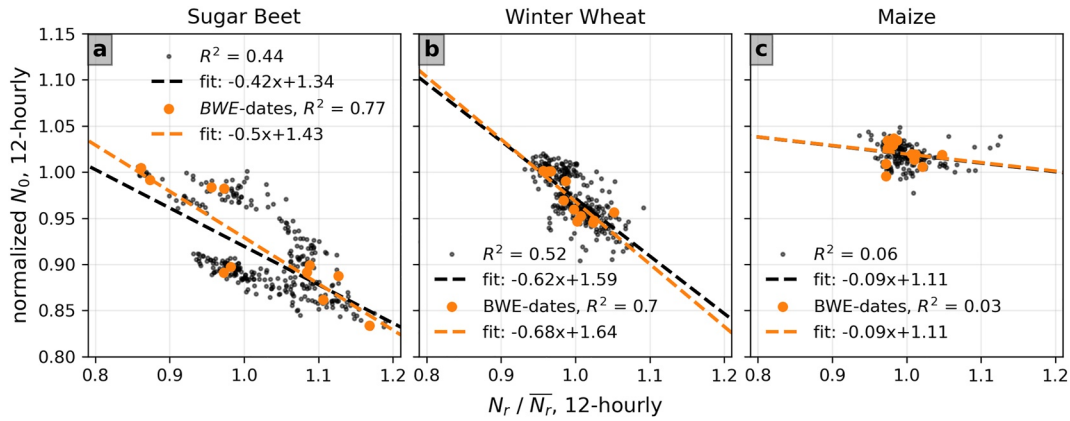

Figure 7. Relationships between N_r normalized with the average N_r of the whole time series and normalized N_0 ($N_0/N_{0,bare}$). Additionally, the relationships when using the biomass sampling dates (orange) only are shown. Except for the relationship for maize considering only the times of BWE measurements, all linear regressions have slopes that are significantly different from 0 (i.e., the two-sided p value was <0.05 for tests with the null hypothesis that the slopes are equal to 0).

with the relationship of Baatz et al. (2015) increased CRNS accuracy compared to the worst-case calibration (i.e., strategy B), but was much higher in comparison to the linear regression models (Figure 6), even when BWE_{tot} (Equation 19, RMSE of 0.048 m^3/m^3) was used instead of BWE_a (Equation 18, RMSE of 0.071 m^3/m^3). As the empirical correction proposed by Baatz et al. (2015) greatly relies on forest biomass data, it implicitly considers a root-shoot ratio valid for trees (i.e., in the order of ∼0.2–0.6; Mokany et al., 2006). In contrast, the root-shoot ratio of crops changes with time. Sugar beet, e.g., showed an increase from ∼0.2 to ∼6 for the root-shoot ratio. Therefore, the root biomass is not adequately represented by the relationship of Baatz et al. (2015). For maize, the relationship of Baatz et al. (2015) resulted in a decreased accuracy due to the additional neutron scattering processes discussed earlier.

3.4. Soil Moisture Content Correction With the Neutron Ratio

We also investigated the possibility of using N_r for the correction of CRNS-derived soil moisture content (Jakobi et al., 2018; Tian et al., 2016; Vather et al., 2020). For this, we established linear regression models between N_0 and N_r (Figure 7) using all measurements from the observation period (Figure 7, black) and measurements on biomass measurement dates only (Figure 7, orange). For sugar beet (Jakobi et al., 2018) and winter wheat, linear relationships between N_r and N_0 were found when considering the whole measurement period (Figures 7a and 7b). For maize, a much flatter regression slope was found (Figure 7c) and the R^2 was also lower (0.06) compared to sugar beet (0.44) and winter wheat (0.52). If only days with in-situ BWE samples were considered, the R^2 for sugar beet (0.77) and winter wheat (0.70) increased, while the R^2 for maize decreased to 0.03. Except for maize with in-situ biomass sample times only, all slopes were significantly different from 0 ($p < 0.05$).

The linear regression models for predicting N_0 from N_r were also used for the correction of soil moisture content estimates using Equation 16 (Figure 8). For all three crop types, the soil moisture content estimates obtained using a correction based on N_r were more accurate than the estimates obtained using calibration strategy B as indicated by the lower RMSE of 0.032, 0.022 and 0.011 m^3/m^3 for sugar beet, winter wheat and maize, respectively. If only N_r values at times of biomass measurements were used to derive the correction models (Figure 7, orange), similar results were obtained except for maize due to the insignificant regression model (Figure 7c).

3.5. Soil Moisture Content Correction With Thermal Neutrons

In a next step, we investigated the possibility of using the thermal neutron intensity for the correction of biomass effects on soil moisture content estimation with CRNS. For this, we established linear regression models for predicting the change in the calibration parameter N_0 from the thermal neutron intensity using all measurements from the observation periods (Figure 9, black) and measurements from the biomass measurement dates only (Figure 9, orange). All three crop types showed linear $T - N_0$ relationships like the relationships between BWE_{tot}

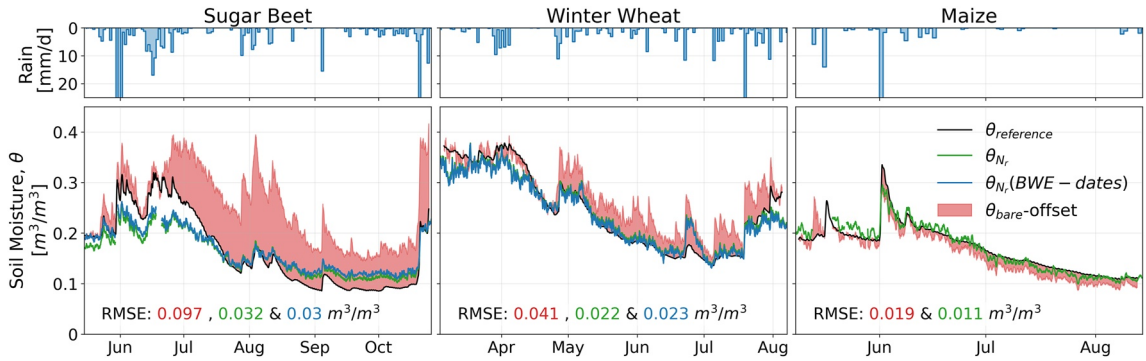

Figure 8. Times series of the cosmic-ray neutron sensor (CRNS)-derived soil moisture content corrected with N_r (green, strategy C) and N_r obtained during times of biomass sampling (blue, strategy C). For comparison, the vertically and horizontally weighted reference soil moisture content (black) and the offset resulting from bare soil calibration of the CRNS (red, strategy B) are also shown.

and N_0 (Figure 5), with sugar beet showing the steepest regression slope and maize showing a positive relationship between T and N_0. When only the biomass measurement dates were used, higher correlations were obtained (Figures 9a–9c). However, the regression results were similar to the case where all data were considered.

Subsequently, the linear regression models for predicting the change in N_0 from the thermal neutron intensity were used for correcting CRNS soil moisture content estimates using Equation 17 (Figure 10). For all three crop types, the correction using thermal neutrons produced better results than the calibration strategy B as indicated by the decrease in RMSE to 0.017, 0.019, and 0.009 m^3/m^3 for sugar beet, winter wheat, and maize, respectively. The results were similar when the linear regression models based only on days with biomass measurements were considered (Figure 9, orange).

3.6. Biomass Estimation From the Neutron Ratio

After evaluating different approaches for correcting soil moisture content estimates, we now evaluate the potential of N_r for estimating crop biomass development (Andreasen, Jensen, Desilets, Zreda, et al., 2017; Jakobi et al., 2018; Tian et al., 2016). The N_r for sugar beet was linearly correlated with in-situ measured BWE_a (Figure 11a; Jakobi et al., 2018). In contrast, the linear regressions for winter wheat and maize did not indicate significant slopes (i.e., the two-sided p values for a test with the null hypothesis that the slopes are equal to 0 were >0.05, Figures 11b and 11c). This means that the prediction of aboveground biomass from N_r was not possible for winter wheat and maize in our study. Tian et al. (2016) and Vather et al. (2020) suggested to use

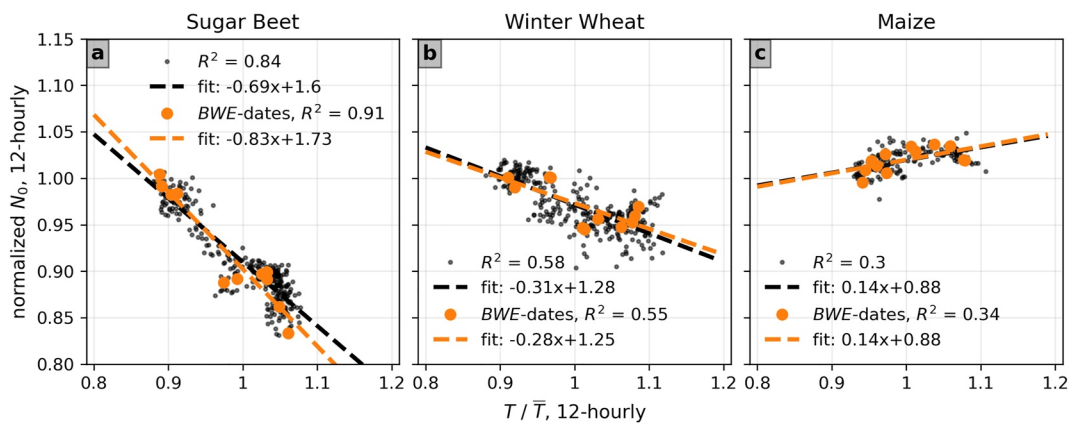

Figure 9. Relationship between normalized thermal neutron intensity (T) normalized with the average T of the whole time series and normalized N_0 ($N_0/N_{0,bare}$) for (a) sugar beet, (b) winter wheat, and (c) maize (black). Additionally, the relationships if only observations at dates of biomass water equivalent (BWE) sampling (orange) were considered are shown. The slopes of all regression models were significantly different from 0 (i.e., the two-sided p value was <0.05 for tests with the null hypothesis that the slopes are equal to 0).

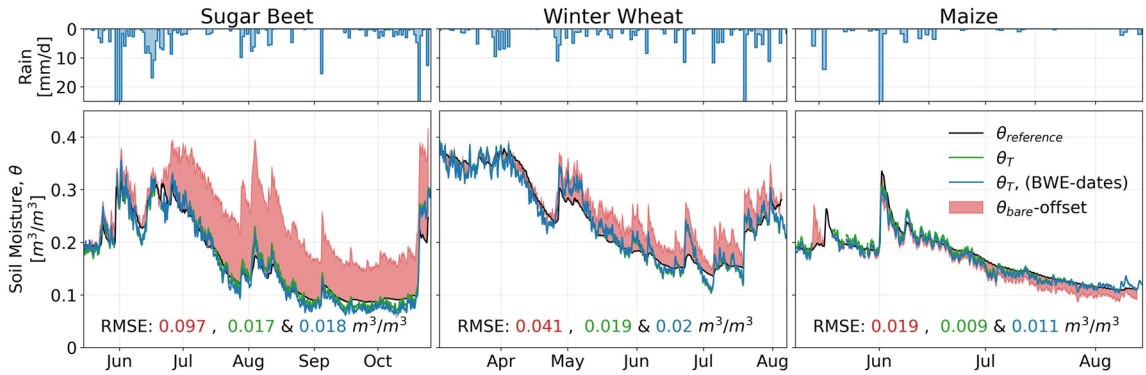

Figure 10. Times series of the cosmic-ray neutron sensor (CRNS)-derived soil moisture content corrected with thermal neutrons (green, strategy C) and with thermal neutrons obtained during dates of biomass sampling (blue, strategy C). For comparison, the vertically and horizontally weighted reference soil moisture content (black) and the offset obtained from bare soil calibration (red, strategy B) are shown.

uncorrected thermal and epithermal neutron intensities for the derivation of the N_r. However, this reduced the R^2 of the N_r-BWE_a relationship from 0.12 to 0.00 for winter wheat and from 0.92 to 0.73 for sugar beet, while it increased R^2 only slightly for maize (from 0.02 to 0.04). It has to be noted that an outlier was removed for sugar beet (Figure 11a, circle with dot; also see Jakobi et al., 2018). If this measurement was included in the analysis, the R^2 was reduced to 0.68.

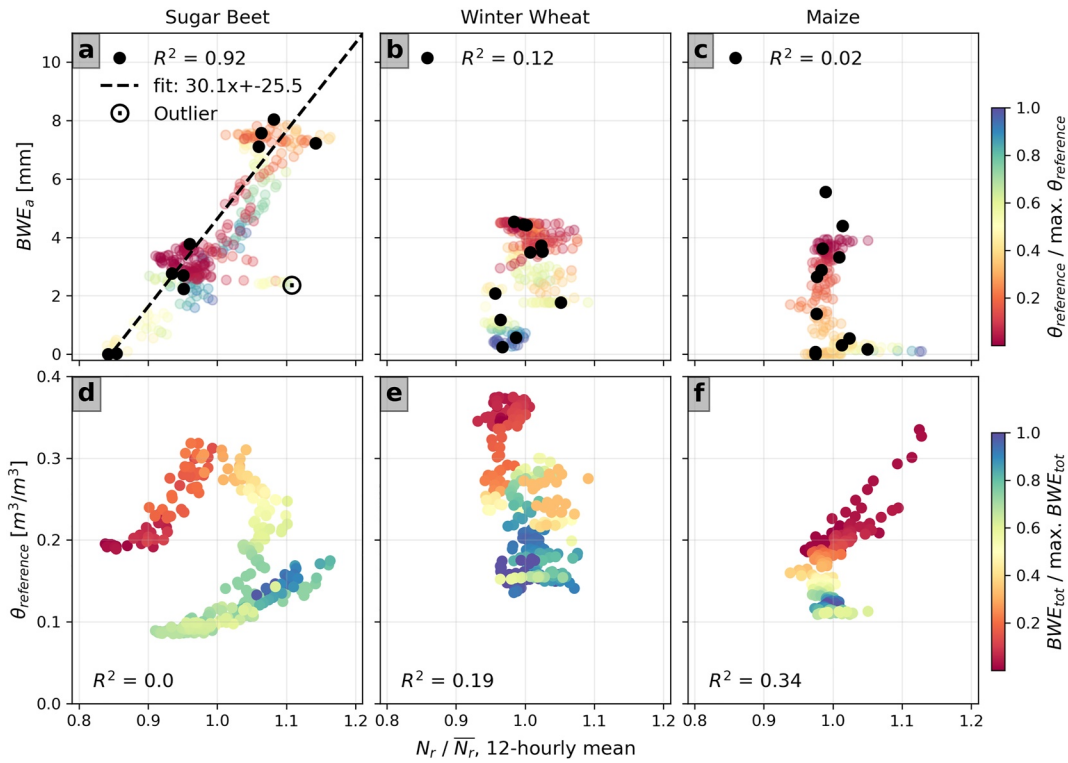

Figure 11. Relationships of neutron ratio (N_r) normalized with the average N_r of the whole time series and measured aboveground biomass water equivalent (BWE_a) of (a) sugar beet, (b) winter wheat, and (c) and maize and relationships of N_r with horizontally and vertically weighted reference soil moisture content ($\theta_{reference}$) for (d) sugar beet, (e) winter wheat, and (f) maize, respectively. The coloring sequences in subplots (a)–(c) indicate changes in $\theta_{reference}$. The coloring sequences in subplots (c)–(f) indicate changes in BWE_{tot} (linearly interpolated). Additionally, the linear regression model for deriving BWE_a from N_r for the Sugar Beet experiment is shown. The slopes of the linear regressions were significantly different from 0 for the relationships presented in subplots (a), (e), and (f) (i.e., the two-sided p value was <0.05 for a test with the null hypothesis that the slope is equal to 0).

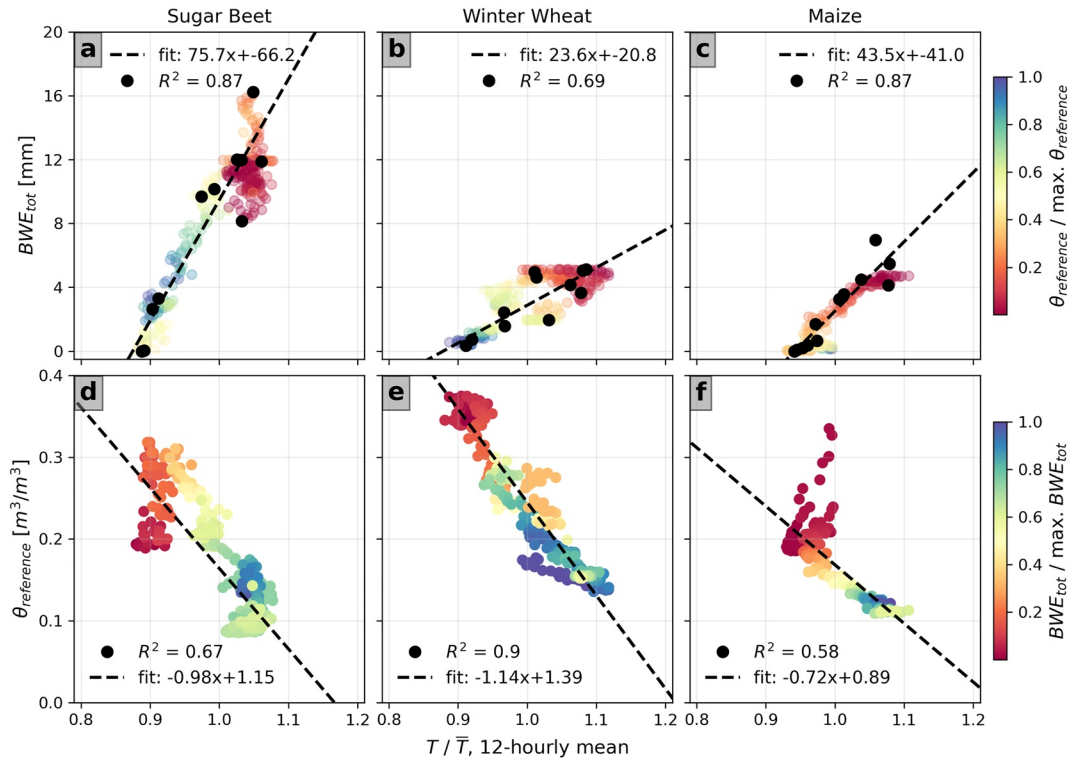

Figure 12. Scatter plots of thermal neutron intensity (T) normalized with the average T of the whole time series and BWE_{tot} as well as normalized T and the reference soil moisture content ($\theta_{reference}$) for (a, d) sugar beet, (b, e) winter wheat, and (c, f) maize. The coloring sequence in subplots (a–c) indicate changes in $\theta_{reference}$. The coloring sequence in subplots (c–f) indicate changes in BWE_{tot} (linearly interpolated). All linear regressions have slopes that are significantly different from 0 (i.e., the two-sided p value was <0.05 for tests with the null hypothesis that the slopes are equal to 0).

Because N_r could also be influenced by changes in soil moisture content, we also investigated the N_r-soil moisture content relationship. However, we found only weak relationships for all three crops that could not be well described with linear or exponential models (Figures 11d–11f). For winter wheat and maize, the slopes of the linear regressions were significantly different from 0 (i.e., two-sided $p < 0.05$, Figures 11e and 11ure 11f). However, the low R^2-values (≤0.34) indicated only weak dependencies. For sugar beet, the R^2 was 0.00. These results confirm previous findings by Tian et al. (2016) and Andreasen, Jensen, Desilets, Zreda, et al. (2017) that the N_r is only weakly related to soil moisture content.

We observed hysteretic behavior in the soil moisture content-N_r relationship for sugar beet (Figure 11d). Similarly, the N_r-N_0 relationship also showed hysteresis (Figure 7a). The color sequence showing the development of BWE_{tot} (Figure 11d) indicates that the hysteresis could be related to sugar beet growth, which is also characterized by changes in plant structure (e.g., development of leaves and tap roots). However, the hysteresis could also be an effect of the soil (and plant) heterogeneity in field F01 (shown in Figure 1 in Jakobi et al., 2018), which may affect thermal and epithermal neutron intensities differently due to the different radial footprints. We also tested if BWE_b or BWE_{tot} for sugar beet could be predicted from N_r, but found lower R^2 values (0.35 and 0.73, respectively) in comparison to the R^2 calculated between N_r and BWE_a (0.92, Figure 11a).

3.7. Biomass Estimation From Thermal Neutrons

Finally, we investigated the potential of T for estimating biomass of the considered crops (Figures 12a–12c). For all three crop types, T was linearly related with in-situ measured BWE_{tot}. R^2 was lowest for winter wheat (0.69), while it was 0.87 for sugar beet and maize. The steepest regression slope was obtained for sugar beet, while the slopes for maize and especially for winter wheat were much lower. For sugar beet, the R^2 was slightly lower compared to the R^2 that was found for predicting BWE_a from N_r. For winter wheat, the relatively low R^2 may be related to the large equipment island, where only a thin grass cover was present and no crops were growing. Thus,

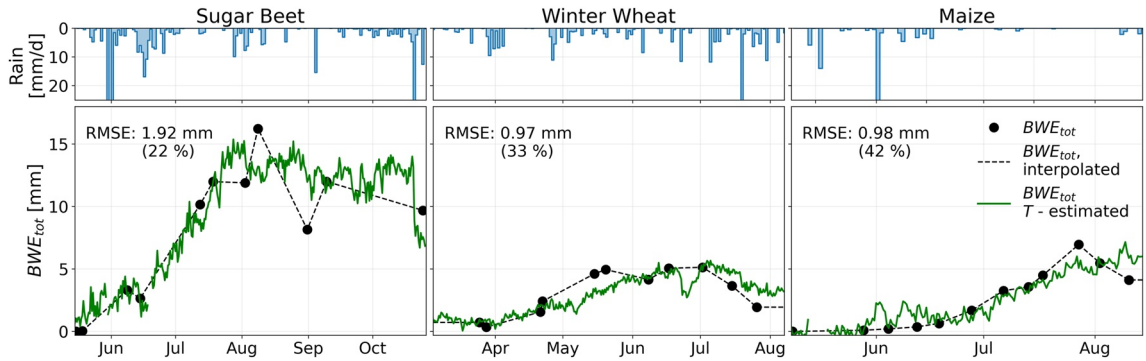

Figure 13. Time series of precipitation and the measured (black dots), interpolated (striped lines), and thermal neutron (T) estimated (green lines) sum of the aboveground and belowground biomass water equivalent (BWE_{tot}) for sugar beet, winter wheat, and maize. Furthermore, the root mean square error (RMSE) and the RMSE relative to the average interpolated BWE_{tot} are provided.

soil moisture content may have been of greater importance for the thermal neutron intensity in the case of winter wheat as compared to sugar beet and maize.

The scatter plots (Figures 12d–12f) suggest that the thermal neutron intensity is influenced by soil moisture content, which seems to contradict our findings above. However, this apparent dependence of thermal neutron intensity on soil moisture content may partly be explained by the fact that for our experiments the increase of biomass usually coincides with decreasing soil moisture content due to the increasing water demand of the crops (see Figures 2e and 2f). This could also be the reason why for our experiments, the epithermal neutron intensities and biomass correlated reasonably well (i.e., R^2 was 0.1, 0.61, and 0.85 for sugar beet, winter wheat, and maize, respectively). However, there are periods where the thermal neutron intensity stayed almost constant during bare soil conditions, while the reference soil moisture content increased considerably (Figure 12d, with T ~0.9 and $\theta_{reference}$ ~0.2–0.3 m^3/m^3, and Figure 12f with T ~0.95 and $\theta_{reference}$ ~0.2–0.3 m^3/m^3) indicating that thermal neutron intensity was more influenced by vegetation than by soil moisture content.

Since all relationships were significant, the linear regression models from Figures 12a–12c were used for estimating temporally variable BWE_{tot} for all three crop types (Figure 13). The RMSE indicated an estimation accuracy of 1.92, 0.97, and 0.98 mm for sugar beet, winter wheat, and maize, respectively, which corresponded to 22%, 33%, and 42% of the average interpolated BWE_{tot}. Larger deviations were mostly associated with precipitation events, which sometimes resulted in a decrease of the thermal neutron intensity and thus underestimated BWE_{tot} (e.g., at the end of the measurement period of sugar beet). In other periods, the thermal neutron intensity and thus BWE_{tot} increased with precipitation (e.g., beginning of June for maize). For winter wheat, BWE_{tot} was systematically underestimated from the end of April until the beginning of June and overestimated from the beginning of July until the end of the observation period (Figure 13). These deviations can also be identified in Figure 12b (with T ~1 and BWE ~2–4 mm) and can possibly be explained with a change in plant structure in the growing season.

4. Discussion

4.1. Correction of Biomass Effects on Soil Moisture Content Estimates With CRNS

The strategies for correcting soil moisture content estimates with CRNS for biomass effects, the associated measurement requirements, and the resulting RMSE are summarized in Table 3. We found that correcting the epithermal neutron intensities based on local linear regression models between N_0 and BWE, N_r or the thermal neutron intensity led to improved performance compared to the widely used bare soil calibration (e.g., Baatz et al., 2014; Bogena et al., 2018; Cooper et al., 2021; Hawdon et al., 2014; Zreda et al., 2012). Considering in-situ measured BWE_{tot} always resulted in the most accurate CRNS-based soil moisture content estimates, but this requires several reference soil moisture content and biomass measurements during the growing season. The second highest accuracy was achieved when thermal neutron intensity was used for correction (see Table 3). This correction approach only requires thermal neutron and soil moisture content measurements. However, the corresponding regression coefficients (see Figure 9) are plant specific. In addition, we expect the coefficients to be site-specific due to the

Table 3
Calibration/Correction Strategies, Measurement Requirements, and Associated Root Mean Square Error (RMSE) of the CRNS Derived Soil Moisture Content Estimations for the Three Crops

Calibration/Correction strategy	Measurement requirements (in addition to epithermal CRNS measurements)	Sugar beet	Winter wheat	Maize
		RMSE [m^3/m^3]		
Optimized (no correction, strategy a)	Multiple in-situ soil moisture contents (here continuous measurements)	0.042	0.031	0.011
Bare soil (no correction, strategy b)	One in-situ soil moisture content in the beginning of the measurement	0.097	0.041	0.019
BWE_a	Multiple aboveground biomasses and in-situ soil moisture contents measured at the same time	0.032	0.018	0.009
BWE_{tot}	Multiple total biomasses and in-situ soil moisture contents measured at the same time	0.015	0.018	0.009
$BWE_{a, Baatz}$	One in-situ soil moisture content with low aboveground biomass and multiple aboveground biomasses	0.071	0.027	0.027
$BWE_{tot, Baatz}$	One in-situ soil moisture content with low total biomass and multiple total biomasses	0.048	0.026	0.029
N_r (N_r at BWE-dates)	Multiple in-situ soil moisture contents and thermal neutron detectors	0.032 (0.03)	0.022 (0.023)	0.011 (–)
T (T at BWE-dates)	Multiple in-situ soil moisture contents and thermal neutron detectors	0.017 (0.018)	0.019 (0.02)	0.009 (0.011)

Note. Green and orange highlight the best and second-best performance, respectively, and red highlights the worst performance in RMSE.

absorption of thermal neutrons on soil minerals. Even though N_r was insensitive to biomass changes of winter wheat and maize in this study, the accuracy achieved using a correction based on N_r was similar to the accuracy achieved with in-situ measured aboveground biomass with the added advantage that no in-situ biomass information is required (see Table 3; Jakobi et al., 2018; Tian et al., 2016; Vather et al., 2020). The empirical relation of Baatz et al. (2015) also resulted in a considerable improvement in accuracy for sugar beet and winter wheat, and the performance could possibly be improved if an exponential instead of a linear model would be considered (e.g., Hawdon et al., 2014). However, the relation of Baatz et al. (2015) failed to represent the effect of maize biomass on the epithermal neutron intensity, because of the observed increase in N_0 with increasing biomass (see Figure 5). Nevertheless, considering the biomass effect on CRNS-based soil moisture content estimates through this type of generic empirical model is still appealing because it only requires biomass estimates and no soil moisture content measurements are required (Table 3; Baatz et al., 2015; Hawdon et al., 2014).

The improved accuracy of the soil moisture content estimates after correction using the thermal neutron intensity or N_r may potentially also be explained by the shallower penetration depth of thermal neutrons (Jakobi et al., 2021) compared to epithermal neutrons (Franz et al., 2012; Köhli et al., 2015; Schrön et al., 2017). It is possible that the corrections considering thermal neutrons (i.e., also N_r) compensate for the vertical soil moisture content heterogeneity. To this end, reference soil moisture content information in depths <5 cm was not available in our experiments and thus not considered in the vertical weighting function for epithermal neutrons of Schrön et al. (2017). This would be consistent with earlier studies that reported the strong influence of vertical soil moisture content heterogeneity on the accuracy of soil moisture content estimation from epithermal neutrons (Baroni et al., 2018; Franz, Zreda, Ferre, & Rosolem, 2013; Scheiffele et al., 2020) and suggested to additionally install point sensors for estimating a field-representative shape of the soil moisture content profile (Baroni et al., 2018; Scheiffele et al., 2020; Sigouin et al., 2016).

4.2. Biomass Estimation With CRNS

The experiments with three crop types showed that N_r could not generally be used for the prediction of aboveground biomass, as suggested in earlier studies (Andreasen, Jensen, Desilets, Zreda, et al., 2017; Jakobi et al., 2018; Tian et al., 2016; Vather et al., 2020). The estimation of aboveground biomass from N_r was possible for sugar beet, but not for winter wheat and maize in this study (Figure 11). In contrast, the estimation of total biomass (aboveground and belowground biomass) from thermal neutron intensity alone was possible for all investigated crops. However, the empirical relationships between thermal neutron intensity and biomass varied considerably between the three crops (Figures 12a–12c). A possible explanation for this could be a variation in soil chemistry that affected the

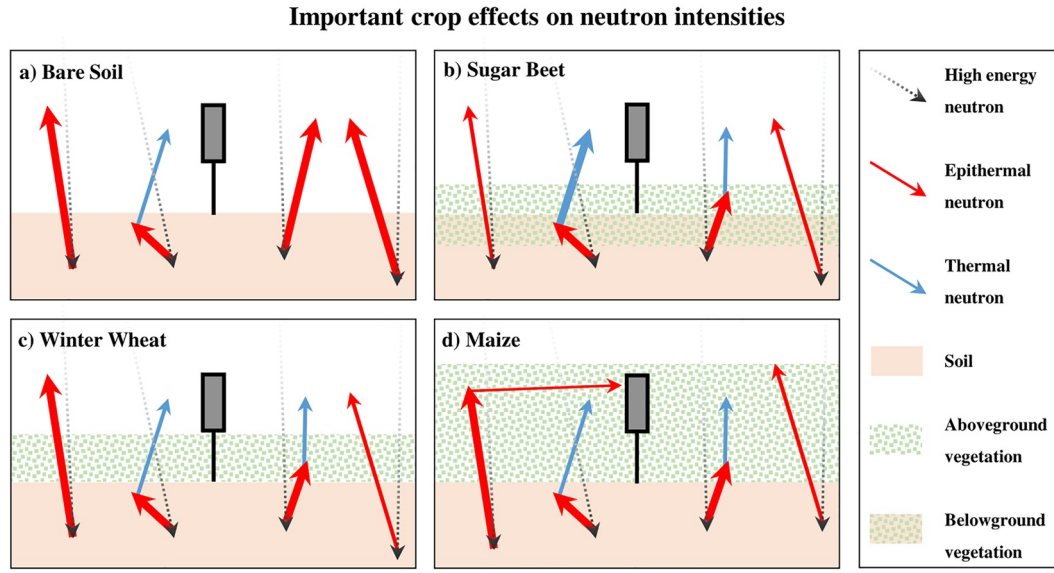

Figure 14. Summary of important vegetation related processes for thermal and epithermal neutrons for (a) bare soil, (b) sugar beet, (c) winter wheat, and (d) maize. The thickness of the blue and red arrows qualitatively indicates the effects on the measured neutron intensities.

intensity of the thermal neutrons differently for the three investigated fields (Zreda et al., 2008). However, this is unlikely as the three fields are very close to each other and with the same geology, so that the differences in soil chemistry are only marginal. Therefore, we assume that the relationship between the thermal neutron intensity and biomass is mainly plant-specific, that is, influenced by plant structure.

Furthermore, we found that the observed correlation between thermal neutron intensity and soil moisture content (Figures 12d–12f) is apparent due to the simultaneous development of biomass. This finding is supported by the study of Tian et al. (2016) in which thermal neutron intensity also increased mainly with increasing biomass (see Figure 4 in Tian et al., 2016). Since snow is expected to affect thermal neutron intensity in a similar way as vegetation cover, our interpretations are also supported by findings from Desilets et al. (2010). They showed that the thermal neutron intensity increased strongly with the onset of snow precipitation, while the epithermal neutron intensity decreased. This finding was verified using neutron transport simulations, where a ∼2.5-fold increase in thermal neutron intensity for increasing snow thickness up to ∼3 g/cm^2 was found as compared to snow-free conditions (see Figure 4 in Zweck et al., 2013). In contrast, the reduction in thermal neutron intensity due to increasing soil moisture content from ∼0.10 to 0.45 m^3/m^3 can be approximated from neutron transport simulations presented in Figure 2 of Zreda et al. (2008) and is expected to amount up to ∼20% only, depending on soil chemistry. In addition, unpublished results from neutron transport simulations indicate an increase in thermal neutron intensity with increasing soil moisture content up to ∼0.15 m^3/m^3, followed by a stable to moderately decreasing thermal neutron intensity with increasing soil moisture content (pers. communication Daniel Rasche; also see Figure 1 in Jakobi et al., 2021). Consequently, the thermal neutron intensity should be affected more strongly by crop biomass than soil moisture content, thus opening the possibility of biomass estimation from thermal neutron intensity as shown in our study.

4.3. Vegetation Influence on Neutron Intensities

Figure 14 summarizes important vegetation-related processes controlling the epithermal and thermal neutron intensity. In case of bare soil conditions (Figure 14a), thermal neutrons are mainly produced in the ground. In the case where vegetation is present, the epithermal neutron intensity is decreased by moderation of biomass, resulting in additional production of thermal neutrons (Figure 14c). Moreover, when large amounts of belowground biomass are present (e.g., as for sugar beet), thermal neutron production and epithermal moderation in the ground are additionally enhanced (Figure 14b). When the detector is surrounded by tall vegetation (e.g., as for maize), the greater density of scattering centers (i.e., atomic nuclei of the biomass) increases the local neutron density,

resulting in a higher neutron detection probability (pers. communication Markus Köhli). This phenomenon was observed for maize in this study (Figure 5c), but not for the other crops. This indicates that the neutron intensity also depends on the vegetation structure and the detector position relative to the vegetation. Finally, it should be noted that aggregating the neutron counts to longer time intervals (e.g., daily averages) would not mask the effects of the relatively slow biomass changes of growing vegetation. Therefore, the approaches for biomass corrections explored in this study can also be applied to data from less sensitive standard CRNS.

5. Conclusions and Outlook

In our study, we used soil moisture networks in sugar beet, winter wheat, and maize, to analyze the effect of crop biomass on estimating soil moisture content with CRNS. We found that correcting the influence of vegetation using local linear regression models based on the calibration parameter N_0 consistently improved the accuracy of soil moisture measurements with CRNS. The best performance in terms of RMSE was obtained when both the aboveground and the belowground biomass were considered for correction. When only the aboveground biomass was considered, the performance decreased when high amounts of belowground biomass were present (i.e., in the case sugar beet). The empirical linear relationship of Baatz et al. (2015) also improved measurement accuracy, except for maize where the accuracy was considerably lower after correction. In contrast, a vegetation correction based on the thermal-to-epithermal neutron ratio (N_r) or thermal neutron intensity always improved the accuracy of soil moisture content measurement with CRNS. Different from results presented in earlier studies (Jakobi et al., 2018; Tian et al., 2016), N_r was not consistently related to changes in aboveground biomass. However, we found that the thermal neutron intensity could also be used to predict changes in the total biomass (i.e., the sum of aboveground and belowground biomass water equivalent—BWE_{tot}).

We suggest that future studies investigate the dependency of thermal neutrons on different biomass and vegetation structures in more detail. To this end, irrigation experiments or neutron transport simulations could be used to investigate changes in neutron intensities with constant soil moisture content and to change biomass/vegetation structures (and vice versa). The influence of the vegetation structure (i.e., the density of stalks, fruit bodies, and the plant height) should also be investigated using neutron transport modeling. Similarly, forest sites are interesting to consider as we anticipate a different behavior of thermal neutrons in comparison to sites where all hydrogen sources are at the same height or below the detectors (Andreasen, Jensen, Desilets, Zreda, et al., 2017; Andreasen et al., 2020; Jakobi et al., 2021).

Data Availability Statement

The data sets used in this study and the scripts for processing and plotting of the data can be retrieved from https://doi.org/10.34731/qb7h-6287.

Acknowledgments
The authors thank Daniel Dolfus, Bernd Schilling, Ansgar Weuthen, Nicole Adels, Philip Pohlig, Yasemin Bas, and Odilia Esser for the technical support, the help during installations and the support with labor-intensive tasks such as soil and biomass measurements and sample processing. Furthermore, the authors thank Daniel Rasche, Markus Köhli, and Till Francke for fruitful discussions. The position of Jannis Jakobi was funded by the Deutsche Forschungsgemeinschaft (DFG, German Research Foundation), project 357874777 of the research unit FOR 2694 Cosmic Sense. The authors also received support from SFB-TR32 Patterns in Soil-Vegetation-Atmosphere Systems: Monitoring, Modelling and Data Assimilation funded by the Deutsche Forschungsgemeinschaft (DFG) and TERENO (TERrestrial Environmental Observatories) funded by the Helmholtz-Gemeinschaft. The authors also acknowledge the NMDB database funded by EU-FP7.

References

Andreasen, M., Jensen, K. H., Bogena, H., Desilets, D., Zreda, M., & Looms, M. C. (2020). Cosmic ray neutron soil moisture estimation using physically based site-specific conversion functions. *Water Resources Research*, *56*(11), e2019WR026588. https://doi.org/10.1029/2019WR026588

Andreasen, M., Jensen, K. H., Desilets, D., Franz, T. E., Zreda, M., Bogena, H. R., & Looms, M. C. (2017). Status and perspectives on the cosmic-ray neutron method for soil moisture estimation and other environmental science applications. *Vadose Zone Journal*, *16*(8), vzj2017. https://doi.org/10.2136/vzj2017.04.0086

Andreasen, M., Jensen, K. H., Desilets, D., Zreda, M., Bogena, H. R., & Looms, M. C. (2017). Cosmic-ray neutron transport at a forest field site: The sensitivity to various environmental conditions with focus on biomass and canopy interception. *Hydrology and Earth System Sciences*, *21*(4), 1875–1894. https://doi.org/10.5194/hess-21-1875-2017

Andreasen, M., Jensen, K. H., Zreda, M., Desilets, D., Bogena, H., & Looms, M. C. (2016). Modeling cosmic ray neutron field measurements. *Water Resources Research*, *52*(8), 6451–6471. https://doi.org/10.1002/2015WR018236

Baatz, R., Bogena, H. R., Hendricks Franssen, H.-J., Huisman, J. A., Montzka, C., & Vereecken, H. (2015). An empirical vegetation correction for soil water content quantification using cosmic ray probes. *Water Resources Research*, *51*(4), 2030–2046. https://doi.org/10.1002/2014WR016443

Baatz, R., Bogena, H. R., Hendricks Franssen, H.-J., Huisman, J. A., Qu, W., Montzka, C., & Vereecken, H. (2014). Calibration of a catchment scale cosmic-ray probe network: A comparison of three parameterization methods. *Journal of Hydrology*, *516*, 231–244. https://doi.org/10.1016/j.jhydrol.2014.02.026

Baret, F., Olioso, A., & Luciani, J. L. (1992). Root biomass fraction as a function of growth degree days in wheat. *Plant and Soil*, *140*(1), 137–144. https://doi.org/10.1007/BF00012815

Baroni, G., & Oswald, S. E. (2015). A scaling appro]ch for the assessment of biomass changes and rainfall interception using cosmic-ray neutron sensing. *Journal of Hydrology*, *525*, 264–276. https://doi.org/10.1016/j.jhydrol.2015.03.053

Baroni, G., Scheiffele, L. M., Schrön, M., Ingwersen, J., & Oswald, S. E. (2018). Uncertainty, sensitivity and improvements in soil moisture estimation with cosmic-ray neutron sensing. *Journal of Hydrology*, *564*, 873–887. https://doi.org/10.1016/j.jhydrol.2018.07.053

Bogena, H. R., Herbst, M., Huisman, J. A., Rosenbaum, U., Weuthen, A., & Vereecken, H. (2010). Potential of wireless sensor networks for measuring soil water content variability. *Vadose Zone Journal*, *9*(4), 1002–1013. https://doi.org/10.2136/vzj2009.0173

Bogena, H. R., Herrmann, F., Jakobi, J., Brogi, C., Ilias, A., Huisman, J. A., et al. (2020). Monitoring of snowpack dynamics with cosmic-ray neutron probes: A comparison of four conversion methods. *Frontiers in Water*, *2*, 19. https://doi.org/10.3389/frwa.2020.00019

Bogena, H. R., Huisman, J. A., Baatz, R., Hendricks Franssen, H.-J., & Vereecken, H. (2013). Accuracy of the cosmic-ray soil water content probe in humid forest ecosystems: The worst case scenario. *Water Resources Research*, *49*(9), 5778–5791. https://doi.org/10.1002/wrcr.20463

Bogena, H. R., Huisman, J. A., Güntner, A., Hübner, C., Kusche, J., Jonard, F., et al. (2015). Emerging methods for noninvasive sensing of soil moisture dynamics from field to catchment scale: A review. *WIREs Water*, *2*(6), 635–647. https://doi.org/10.1002/wat2.1097

Bogena, H. R., Huisman, J. A., Schilling, B., Weuthen, A., & Vereecken, H. (2017). Effective calibration of low-cost soil water content sensors. *Sensors*, *17*(1), 208. https://doi.org/10.3390/s17010208

Bogena, H. R., Montzka, C., Huisman, J. A., Graf, A., Schmidt, M., Stockinger, M., et al. (2018). The TERENO-Rur hydrological observatory: A multiscale multi-compartment research platform for the advancement of hydrological science. *Vadose Zone Journal*, *17*(1), 180055. https://doi.org/10.2136/vzj2018.03.0055

Bogena, H. R., Schrön, M., Jakobi, J., Ney, P., Zacharias, S., Andreasen, M., et al. (2021). COSMOS-Europe: A European Network of cosmic-ray neutron soil moisture sensors. *Journal of Earth System Science*, *14*(3), 1125–1151. https://doi.org/10.5194/essd-2021-325

Brogi, C., Huisman, J. A., Herbst, M., Weihermüller, L., Klosterhalfen, A., Montzka, C., et al. (2020). Simulation of spatial variability in crop leaf area index and yield using agroecosystem modeling and geophysics-based quantitative soil information. *Vadose Zone Journal*, *19*(1), e20009. https://doi.org/10.1002/vzj2.20009

Brogi, C., Huisman, J. A., Pätzold, S., Hebel, C., vonWeihermüller, L., Kaufmann, M. S., et al. (2019). Large-scale soil mapping using multi-configuration EMI and supervised image classification. *Geoderma*, *335*, 133–148. https://doi.org/10.1016/j.geoderma.2018.08.001

Cooper, H. M., Bennett, E., Blake, J., Blyth, E., Boorman, D., Cooper, E., et al. (2021). COSMOS-UK: National soil moisture and hydrometeorology data for environmental science research. *Earth System Science Data*, *13*(4), 1737–1757. https://doi.org/10.5194/essd-13-1737-2021

Desilets, D., & Zreda, M. (2001). On scaling cosmogenic nuclide production rates for altitude and latitude using cosmic-ray measurements. *Earth and Planetary Science Letters*, *193*(1–2), 213–225. https://doi.org/10.1016/S0012-821X(01)00477-0

Desilets, D., & Zreda, M. (2003). Spatial and temporal distribution of secondary cosmic-ray nucleon intensities and applications to in situ cosmogenic dating. *Earth and Planetary Science Letters*, *206*(1–2), 21–42. https://doi.org/10.1016/S0012-821X(02)01088-9

Desilets, D., Zreda, M., & Ferré, T. P. A. (2010). Nature's neutron probe: Land surface hydrology at an elusive scale with cosmic rays. *Water Resources Research*, *46*(11), W11505. https://doi.org/10.1029/2009WR008726

Dimitrova-Petrova, K., Geris, J., Wilkinson, M. E., Rosolem, R., Verrot, L., Lilly, A., & Soulsby, C. (2020). Opportunities and challenges in using catchment-scale storage estimates from cosmic ray neutron sensors for rainfall-runoff modelling. *Journal of Hydrology*, *586*, 124878. https://doi.org/10.1016/j.jhydrol.2020.124878

Dong, J., Ochsner, T. E., Zreda, M., Cosh, M. H., & Zou, C. B. (2014). Calibration and validation of the COSMOS Rover for surface soil moisture measurement. *Vadose Zone Journal*, *13*(4), 1–8. https://doi.org/10.2136/vzj2013.08.0148

Fersch, B., Francke, T., Heistermann, M., Schrön, M., Döpper, V., Jakobi, J., et al. (2020). A dense network of cosmic-ray neutron sensors for soil moisture observation in a highly instrumented pre-Alpine headwater catchment in Germany. *Earth System Science Data*, *12*(3), 2289–2309. https://doi.org/10.5194/essd-12-2289-2020

Fersch, B., Jagdhuber, T., Schrön, M., Völksch, I., & Jäger, M. (2018). Synergies for soil moisture retrieval across scales from airborne polarimetric SAR, cosmic ray neutron roving, and an in situ sensor network. *Water Resources Research*, *54*(11), 9364–9383. https://doi.org/10.1029/2018WR023337

Franz, T. E., Zreda, M., Ferre, T. P. A., & Rosolem, R. (2013). An assessment of the effect of horizontal soil moisture heterogeneity on the area-average measurement of cosmic-ray neutrons. *Water Resources Research*, *49*(10), 6450–6458. https://doi.org/10.1002/wrcr.20530

Franz, T. E., Zreda, M., Ferre, T. P. A., Rosolem, R., Zweck, C., Stillman, S., et al. (2012). Measurement depth of the cosmic ray soil moisture probe affected by hydrogen from various sources. *Water Resources Research*, *48*(8), W08515. https://doi.org/10.1029/2012WR011871

Franz, T. E., Zreda, M., Rosolem, R., Hornbuckle, B. K., Irvin, S. L., Adams, H., et al. (2013). Ecosystem-scale measurements of biomass water using cosmic ray neutrons. *Geophysical Research Letters*, *40*(15), 3929–3933. https://doi.org/10.1002/grl.50791

Fuchs, H. (2016). *Effects of biomass on soil moisture measurements using cosmic-ray neutron probes (Master Thesis)*. Radboud University, the Netherlands and University of Duisburg-Essen, Germany.

Hawdon, A., McJannet, D., & Wallace, J. (2014). Calibration and correction procedures for cosmic-ray neutron soil moisture probes located across Australia. *Water Resources Research*, *50*(6), 5029–5043. https://doi.org/10.1002/2013WR015138

Jakobi, J., Huisman, J. A., Köhli, M., Rasche, D., Vereecken, H., & Bogena, H. R. (2021). The footprint characteristics of cosmic ray thermal neutrons. *Geophysical Research Letters*, *48*(15), e2021GL094281. https://doi.org/10.1029/2021GL094281

Jakobi, J., Huisman, J. A., Schrön, M., Fiedler, J., Brogi, C., Vereecken, H., & Bogena, H. R. (2020). Error estimation for soil moisture measurements with cosmic ray neutron sensing and implications for rover surveys. *Frontiers in Water*, *2*, 10. https://doi.org/10.3389/frwa.2020.00010

Jakobi, J., Huisman, J. A., Vereecken, H., Diekkrüger, B., & Bogena, H. R. (2018). Cosmic ray neutron sensing for simultaneous soil water content and biomass quantification in drought conditions. *Water Resources Research*, *54*(10), 7383–7402. https://doi.org/10.1029/2018WR022692

Knoll, G. F. (2010). *Radiation detection and measurement*, (4th ed., Vol. xxvi, p. 830). John Wiley.

Köhli, M., Schrön, M., Zreda, M., Schmidt, U., Dietrich, P., & Zacharias, S. (2015). Footprint characteristics revised for field-scale soil moisture monitoring with cosmic-ray neutrons. *Water Resources Research*, *51*(7), 5772–5790. https://doi.org/10.1002/2015WR017169

Korres, W., Reichenau, T. G., Fiener, P., Koyama, C. N., Bogena, H. R., Cornelissen, T., et al. (2015). Spatio-temporal soil moisture patterns – A meta-analysis using plot to catchment scale data. *Journal of Hydrology*, *520*, 326–341. https://doi.org/10.1016/j.jhydrol.2014.11.042

Li, D., Schrön, M., Köhli, M., Bogena, H., Weimar, J., Jiménez Bello, M. A., et al. (2019). Can drip irrigation be scheduled with cosmic-ray neutron sensing?*Vadose Zone Journal*, *18*(1), 190053. https://doi.org/10.2136/vzj2019.05.0053

McJannet, D., Franz, T., Hawdon, A., Boadle, D., Baker, B., Almeida, A., et al. (2014). Field testing of the universal calibration function for determination of soil moisture with cosmic-ray neutrons. *Water Resources Research*, *50*(6), 5235–5248. https://doi.org/10.1002/2014WR015513

Mokany, K., Raison, R. J., & Prokushkin, A. S. (2006). Critical analysis of root: Shoot ratios in terrestrial biomes. *Global Change Biology*, *12*(1), 84–96. https://doi.org/10.1111/j.1365-2486.2005.001043.x

Rasche, D., Köhli, M., Schrön, M., Blume, T., & Güntner, A. (2021). Towards disentangling heterogeneous soil moisture patterns in cosmic-ray neutron sensor footprints. *Hydrology and Earth System Sciences*, *25*(12), 6547–6566. https://doi.org/10.5194/hess-25-6547-2021

Rivera Villarreyes, C. A., Baroni, G., & Oswald, S. E. (2011). Integral quantification of seasonal soil moisture changes in farmland by cosmic-ray neutrons. *Hydrology and Earth System Sciences*, *15*(12), 3843–3859. https://doi.org/10.5194/hess-15-3843-2011

Rosolem, R., Shuttleworth, W. J., Zreda, M., Franz, T. E., Zeng, X., & Kurc, S. A. (2013). The effect of atmospheric water vapor on neutron count in the cosmic-ray soil moisture observing system. *Journal of Hydrometeorology*, *14*(5), 1659–1671. https://doi.org/10.1175/JHM-D-12-0120.1

Rudolph, S., van derKruk, J., Hebel, C., vonAli, M., Herbst, M., Montzka, C., et al. (2015). Linking satellite derived LAI patterns with subsoil heterogeneity using large-scale ground-based electromagnetic induction measurements. *Geoderma*, *241–242*, 262–271. https://doi.org/10.1016/j.geoderma.2014.11.015

Scheiffele, L. M., Baroni, G., Franz, T. E., Jakobi, J., & Oswald, S. E. (2020). A profile shape correction to reduce the vertical sensitivity of cosmic-ray neutron sensing of soil moisture. *Vadose Zone Journal*, *19*(1), e20083. https://doi.org/10.1002/vzj2.20083

Schrön, M., Köhli, M., Scheiffele, L., Iwema, J., Bogena, H. R., Lv, L., et al. (2017). Improving calibration and validation of cosmic-ray neutron sensors in the light of spatial sensitivity. *Hydrology and Earth System Sciences*, *21*(10), 5009–5030. https://doi.org/10.5194/hess-21-5009-2017

Sigouin, M. J., Dyck, M., Si, B. C., & Hu, W. (2016). Monitoring soil water content at a heterogeneous oil sand reclamation site using a cosmic-ray soil moisture probe. *Journal of Hydrology*, *543*, 510–522. https://doi.org/10.1016/j.jhydrol.2016.10.026

Tian, Z., Li, Z., Liu, G., Li, B., & Ren, T. (2016). Soil water content determination with cosmic-ray neutron sensor: Correcting aboveground hydrogen effects with thermal/fast neutron ratio. *Journal of Hydrology*, *540*, 923–933. https://doi.org/10.1016/j.jhydrol.2016.07.004

Topp, G. C., Davis, J. L., & Annan, A. P. (1980). Electromagnetic determination of soil water content: Measurements in coaxial transmission lines. *Water Resources Research*, *16*(3), 574–582. https://doi.org/10.1029/WR016i003p00574

Vather, T., Everson, C. S., & Franz, T. E. (2020). The applicability of the cosmic ray neutron sensor to simultaneously monitor soil water content and biomass in an Acacia mearnsii forest. *Hydrology*, *7*(3), 48. https://doi.org/10.3390/hydrology7030048

Weihermüller, L., Huisman, J. A., Lambot, S., Herbst, M., & Vereecken, H. (2007). Mapping the spatial variation of soil water content at the field scale with different ground penetrating radar techniques. *Journal of Hydrology*, *340*(3–4), 205–216. https://doi.org/10.1016/j.jhydrol.2007.04.013

Zreda, M., Desilets, D., Ferré, T. P. A., & Scott, R. L. (2008). Measuring soil moisture content non-invasively at intermediate spatial scale using cosmic-ray neutrons. *Geophysical Research Letters*, *35*(21), L21402. https://doi.org/10.1029/2008GL035655

Zreda, M., Shuttleworth, W. J., Zeng, X., Zweck, C., Desilets, D., Franz, T., & Rosolem, R. (2012). COSMOS: The cosmic-ray soil moisture observing system. *Hydrology and Earth System Sciences*, *16*(11), 4079–4099. https://doi.org/10.5194/hess-16-4079-2012

Zweck, C., Zreda, M., & Desilets, D. (2013). Snow shielding factors for cosmogenic nuclide dating inferred from Monte Carlo neutron transport simulations. *Earth and Planetary Science Letters*, *379*, 64–71. https://doi.org/10.1016/j.epsl.2013.07.023